

## **PREDICTION OF TWO-DIMENSIONAL DIFFUSION PROBLEMS BASED ON FINITE VOLUME METHOD AND TRIANGULAR UNSTRUCTURED GRID**

Yuttana glasug<sup>1,\*</sup>, Thara Angskun<sup>2</sup> and Keerati Suluksna<sup>1</sup>

<sup>1</sup> School of Mechanical Engineering, Institute of Engineering, Suranaree University of Technology

<sup>2</sup> School of Information Technology, Institute of Social Technology, Suranaree University of Technology

111 University Avenue, Suranare, Muang, Nakorn Ratchasima 30000, Thailand

Tel: 044 224 410, Fax: 044 224 613, \*E-mail: glasug\_yuttana@hotmail.com

### **Abstract**

In engineering applications, the problem geometries are usually found by constructing with complex shapes. Under a condition, it seems to be an impossible thing to solve using analytical methods. As a result, the use of numerical method is a possible way to overcome those problems. This paper presents the numerical method for solving the two-dimensional steady state diffusion. A computer program has been developed based on the finite volume method and triangular unstructured grid arrangement. The considered diffusion problems are governed by the second order PDE equation. They are discretized by using the central differencing scheme. A two-dimensional heat conduction with complex shape have been investigated to assess the reliability of the computer program. The predicted shows that the developed computer program gives a good result compare with the reference data.

**Keywords:** Numerical methods, Diffusion problem, Finite Volume Method, Triangular Unstructured Grid.

### **1. Introduction**

In general, the engineering applications are combined with the complex geometries. This condition is difficult or impossible to solve by using an analytical method. To overcome this problem, the numerical method is employed to solve for an approximation solution rather than those of exact solution. Concept of the numerical method starts from dividing the domain to the finite number of the control volumes (cells). Due to the complex shape of the geometry, however, the use of unstructured mesh is more efficient

than the use of structured mesh as shown in Fig.1. As a result, the unstructured mesh is usually found as a widely use in numerical strategy and will be adopted in the present work.

This paper presents a development of the computer code for predicting of steady two-dimensional diffusion problems. The numerical methodology adopted here is based on finite volume discretization and triangular unstructured grid. This is because the computer program will be extended for CFD development process in the future. The central differencing scheme is used to

discrete the governing equation. Four validation problems are used to assess the computer code.

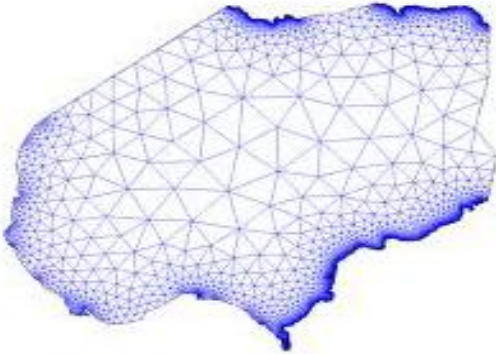


Fig.1 Unstructured mesh for complex geometry.

## 2. Numerical Methodology

### 2.1 Discretization Technique

In general, the governing equation[1] for the diffusion problem can be written in the general form as follows.

$$\text{div}(\Gamma \text{ grad } \phi) + S_\phi = 0 \quad (1)$$

Where  $\Gamma$  denotes the diffusion coefficient,  $\phi$  is the attentive variable and  $S_\phi$  is the source term. Based on the concept of the finite volume method, this governing equation will be integrated over the control volume as follows.

$$\int_{CV} \text{div}(\Gamma \text{ grad } \phi) dV + \int_{CV} S_\phi dV = 0 \quad (2)$$

To determine the diffusion flux throughout the control volume, one can determine on the surface integral rather than volume integral as follows.

$$\sum_i^{\text{surface}} \int_{\Delta A_i} \hat{n}_i \cdot (\Gamma \text{ grad } \phi) dA_i + S_\phi \Delta V = 0 \quad (3)$$

It should be note that the use of surface integral gives a more efficient than those of the volume integral because it is convenient to determine the flux through the cell faces.

### 2.2 Unstructured Mesh Technique

The mashing technique adopted here is the so-called triangular unstructured grid. This mash type consists of three cell faces. After

employing such meshing into Eq.(3), the equation can be written as follows.

$$\sum_i^3 \hat{n}_i \cdot (\Gamma \text{ grad } \phi) \Delta A_i + S_\phi \Delta V = 0 \quad (4)$$

Where  $\Delta A$  is the cell area of face and  $\Delta V$  is the cell volume.

Fig.2 shows the relation between the center node and the neighbor nodes. It can be seen that the relation of those nodes are combined by the unit vectors in normal and tangent directions. The control volume consists of three vertices  $a$ ,  $b$  and  $c$ . it should be noted that those three vertices must be ordered to provide the counterclockwise with respect to the center node. This is necessary to preserve a unique direction of all surface vectors and in this case the outward direction of all unit normal vectors  $\hat{n}$  is attained.

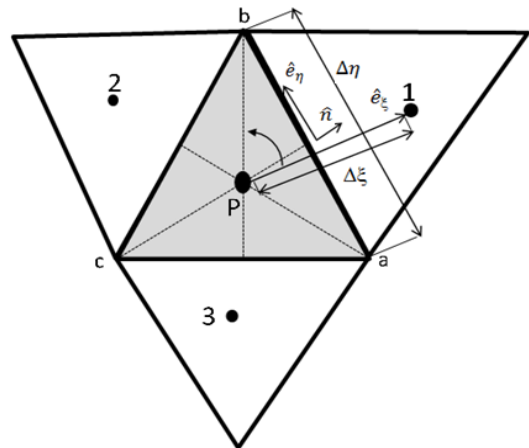


Fig.2 Detail of grid information

The diffusive flux through face  $ab$  can be approximated by using the numerical differencing scheme. In the present work, such approximation has been derived in form of the direct gradient term and the cross-diffusion term as follows.

$$(\Gamma \text{ grad } \phi) \Delta A = \underbrace{\left( \frac{\Gamma}{\Delta \xi} \frac{\hat{n} \cdot \hat{n}}{\hat{n} \cdot \hat{e}_\xi} \Delta A (\phi_b - \phi_P) \right)}_{\text{the direct gradient team}} + \underbrace{\left( -\Gamma \frac{\hat{e}_\xi \cdot \hat{e}_\eta}{\hat{n} \cdot \hat{e}_\xi} \Delta A \left( \frac{\phi_b - \phi_a}{\Delta \eta} \right) \right)}_{\text{the cross-diffusion team}} \quad (5)$$

Where

$$\hat{n} = \frac{\Delta y}{\Delta A} \vec{i} - \frac{\Delta x}{\Delta A} \vec{j} = \frac{y_b - y_a}{\Delta \eta} \vec{i} - \frac{x_b - x_a}{\Delta \eta} \vec{j}$$

$$\hat{e}_\xi = \frac{x_1 - x_p}{\Delta \xi} \vec{i} + \frac{y_1 - y_p}{\Delta \xi} \vec{j}, \text{ and } \hat{e}_\eta = \frac{x_b - x_a}{\Delta \eta} \vec{i} + \frac{y_b - y_a}{\Delta \eta} \vec{j}$$

Eq.(5) can be rearranged as follows:

$$\hat{n} \cdot (\Gamma \text{ grad } \phi) \Delta A = D(\phi_1 - \phi_p) + S \quad (6)$$

Where D is the diffusion coefficient from the direct gradient term and S is the cross-diffusion term which will be treated as the source term.

Substitution the Eq.(6) into Eq.(4), thus

$$\sum_i^3 [D_i(\phi_i - \phi_p) + S_i] + S_\phi \Delta V = 0 \quad (7)$$

It can be seen that Eq.(7) is expressed in the form of linear algebraic equation. The index i represents the running number of the cell faces. After applying Eq.(7) to all faces, the equation can be written as follows:

$$a_p \phi_p = a_1 \phi_1 + a_2 \phi_2 + a_3 \phi_3 + S_1 + S_2 + S_3 + S_\phi V \quad (8)$$

Where

$$a_1 = \frac{\Gamma}{\Delta \xi_1} \frac{\hat{n}_1 \cdot \hat{n}_1}{\hat{n}_1 \cdot \hat{e}_{\xi_1}} \Delta A_1, \quad a_2 = \frac{\Gamma}{\Delta \xi_2} \frac{\hat{n}_2 \cdot \hat{n}_2}{\hat{n}_2 \cdot \hat{e}_{\xi_2}} \Delta A_2$$

$$a_3 = \frac{\Gamma}{\Delta \xi_3} \frac{\hat{n}_3 \cdot \hat{n}_3}{\hat{n}_3 \cdot \hat{e}_{\xi_3}} \Delta A_3, \quad S_1 = -\Gamma \frac{\hat{e}_{\xi_1} \cdot \hat{e}_{\eta_1}}{\hat{n}_1 \cdot \hat{e}_{\xi_1}} \Delta A_1 \left( \frac{\phi_b - \phi_a}{\Delta \eta_1} \right)$$

$$S_2 = -\Gamma \frac{\hat{e}_{\xi_2} \cdot \hat{e}_{\eta_2}}{\hat{n}_2 \cdot \hat{e}_{\xi_2}} \Delta A_2 \left( \frac{\phi_c - \phi_b}{\Delta \eta_2} \right),$$

$$S_3 = -\Gamma \frac{\hat{e}_{\xi_3} \cdot \hat{e}_{\eta_3}}{\hat{n}_3 \cdot \hat{e}_{\xi_3}} \Delta A_3 \left( \frac{\phi_a - \phi_c}{\Delta \eta_3} \right),$$

and  $a_p = a_1 + a_2 + a_3$

Eq.(8) will be applied to all nodes in the domain and then has been solved by Gauss-Seidel relaxation method iteratively.

### 3. Code Validations

#### 3.1 Case A: Square plate with Constant

##### Boundary Values

A two dimensional square plate with a size of  $1 \times 1 \text{ m}^2$  is taken to use as the first problem for assessing an efficiency of the developed code in calculating based on the simple triangular mesh. The boundary conditions of the top side of the square plate is maintained with temperature of  $100^\circ\text{C}$  and the rest sides are subjected to the

temperature of  $0^\circ\text{C}$  as illustrated in Fig.3. The plate made from material with a specified thermal conductivity (k) of  $50 \text{ W/m}^\circ\text{C}$ .

An analytical solution[2] for this problem can be calculated from a following expression.

$$T(x,y) = \sum_{n=1}^{\infty} A_n \sinh(n\pi y) \sin(n\pi x)$$

and  $A_n = 200 \frac{1 - (-1)^n}{n\pi \sinh(n\pi)}$ ;  $n=1,2,3,..$

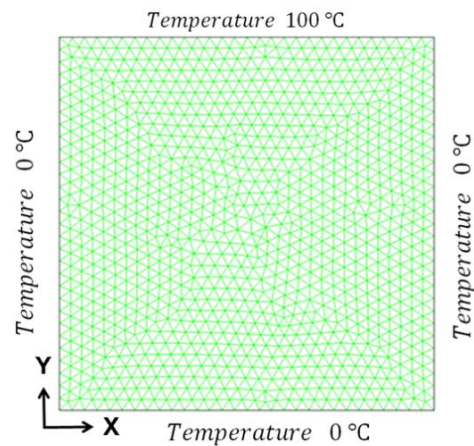


Fig.3 Boundary condition and grid configuration

The numerical prediction is performed on five grid sets with the grid number of 836, 2028, 4924, 14342, and 22518 cells in order to find out the grid independent set. Comparison of the temperature results along the midline  $x=0.5 \text{ m}$  are shown in Fig.4. It can be seen that the predicted results give a very well agree with the analytical solutions.

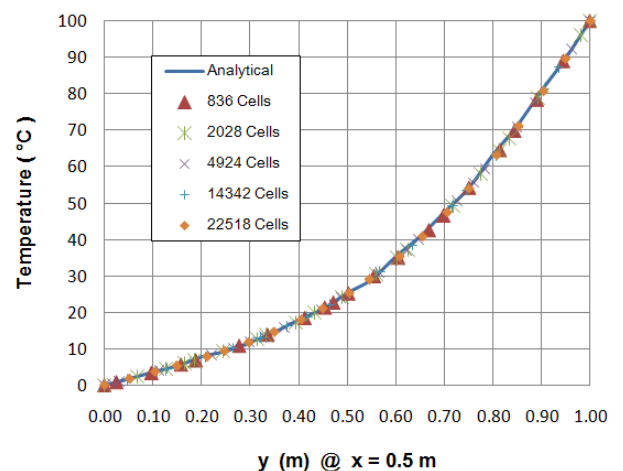


Fig.4 Comparison of temperature for Case A

Fig.5 shows the distribution of the error. It can be seen that the errors are distributed within the range from -0.2% to 0.075%. With the lower density of meshing, the errors trend to shift left to the negative zone but the distribution of the errors trend to spread out. Fig.6 displays the contours of the temperature. It can be seen that the high temperature is produced in the upper zone and then cool down in the lower zone.

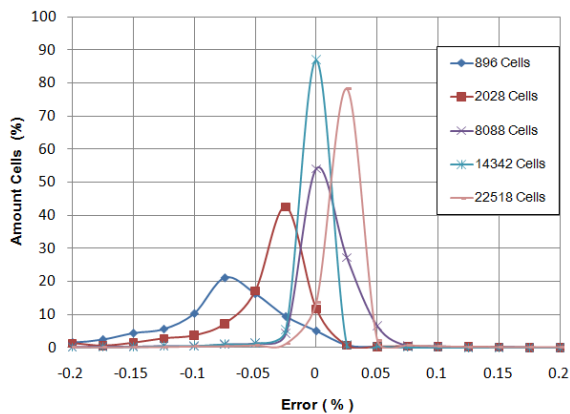


Fig.5 Error distribution of Case A

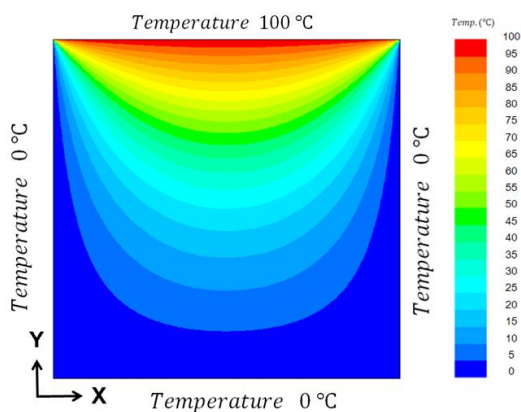


Fig.6 Contours of temperature distribution

### 3.2 Case B: Square Plate with Various Boundary Type

This validated case is constructed with a rectangular plate with the size of  $0.3 \times 0.4 \text{ m}^2$ . This case is set for assessing an efficiency of the developed code on the several of boundary conditions. In this case, the top side of the plate is fixed with a constant temperature (T) of  $100^\circ\text{C}$ .

The left side is subjected a constant heat flux of  $q=500 \text{ kW/m}^2$ . The rest two sides of the plate are set with the condition of insulating as illustrated in Fig.7. The plate made from material with a specified thermal conductivity (k) of  $1000 \text{ W/m}^\circ\text{C}$ .

An analytical solution for this problem can be calculated from a following formulation.

$$T(x,y) = f(x,y) \frac{2q}{kH} + T$$

Where  $f(x,y) = \sum_{n=1}^{\infty} \frac{\sin(a_n H) \cos(a_n y) \cosh(a_n x)}{a_n^2 \sinh(a_n L)}$

and  $a_n = \frac{(2n-1)\pi}{2H}$ ;  $n=1,2,3,..$

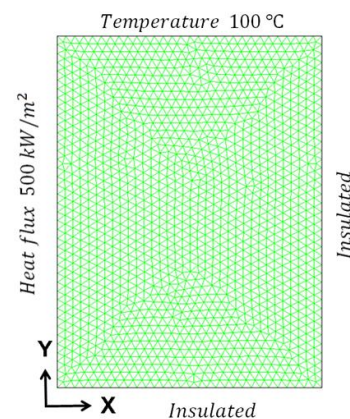


Fig.7 Boundary condition for Case B

Five grid sets of 366, 898, 1414, 6064, and 14426 cells numbers are used to check for the grid independent. Comparison of the temperature results along the midline  $x=0.15 \text{ m}$  are shown in Fig.8. It can be seen that the predicted results give good agreement compared with the exact solutions.

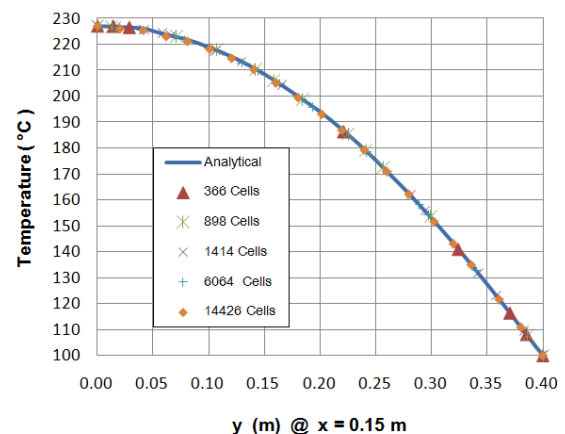


Fig.8 Comparison of temperature for Case B

The error distribution of case B is shown in Fig.9. It can be seen that they are distributed within the range from -0.4% to 0.4%. The lowest density meshing gives positive zone distribution with a more spread out than the finer ones. The temperature distribution is depicted in Fig.10. It can be observed that the high temperature is condensed at the bottom left corner of the plate with the maximum temperature of 280°C. This is because the heat flux on the left side transfers the heat energy inside the plate. The heat energy is protected (no heat lose) by the insulating walls and then distributed to the upper zone.

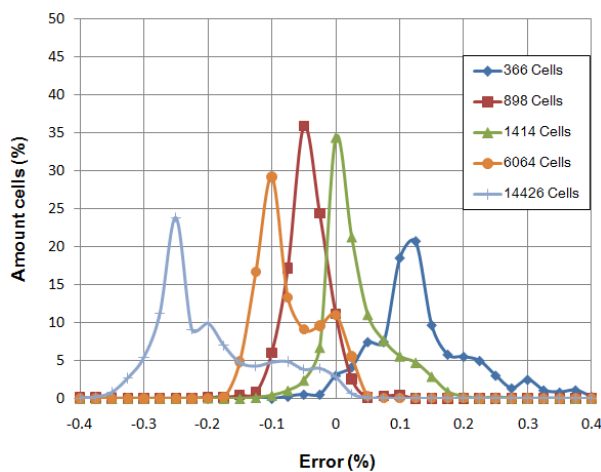


Fig.9 Error distribution of Case B

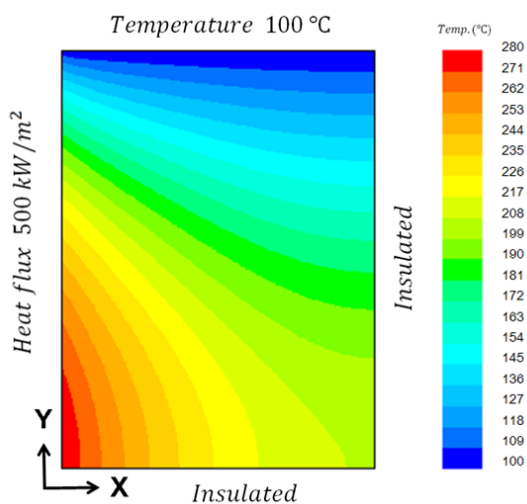


Fig.10 Contour of temperature for Case B

### 3.3 Case C: Diffusion in a Circular Hollow

The diffusion in a circular hollow problem is set for validating the computer code in calculating on the complex geometry. This problem is look like two dimensional donut with the inner ( $R_{in}$ ) and outer ( $R_{out}$ ) radius of 1 and 2 m, respectively. The inner boundary of the hollow is maintained to a constant temperature of 100°C. The outer boundary is subjected to an ambient temperature of 30°C with the heat transfer coefficient ( $h$ ) of 12 W/m<sup>2</sup>. Due to a symmetrical hollow as shown in Fig.11, a haft domain consideration is sufficiently in the process of numerical prediction. As a result, the symmetry plane will be defined with the condition of insulation because no heat transfers across those symmetry planes. In this present, the hollow made from material with a constant thermal conductivity ( $k$ ) of 15 W/m°C.

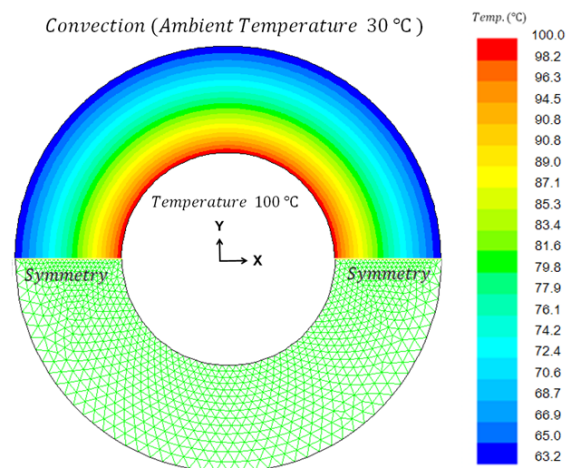


Fig.11 Domain/boundary condition for Case C

The analytical solution[3] of this problem can be calculated from the following equation.

$$T(r) = T_{in} - \frac{f(r)}{C}; r = \sqrt{x^2 + y^2}$$

where  $f(r) = hR_{out}(T_{in} - T_{amb}) \ln\left(\frac{r}{R_{in}}\right)$

and  $C = k + hR_{out} \ln\left(\frac{R_{out}}{R_{in}}\right)$

The grid independent checking of this case is performed based on seven grid test sets corresponding to the cells number of 530, 1848, 3930, 8630, 11548, 16290, and 23796 respectively. Comparison of the temperature along the section line of  $x=0$  m is shown in Fig. 12. It can be seen that the predicted results are satisfactorily with the analytical results. The temperature distribution has a maximum value of  $100^{\circ}\text{C}$  at the inner surface and then reduces to reach a minimum value of 63.2 at the outer surface of the hollow. The temperature contours are illustrated in Fig.11 and the distribution of the errors of each grid sets are displayed in Fig.13.

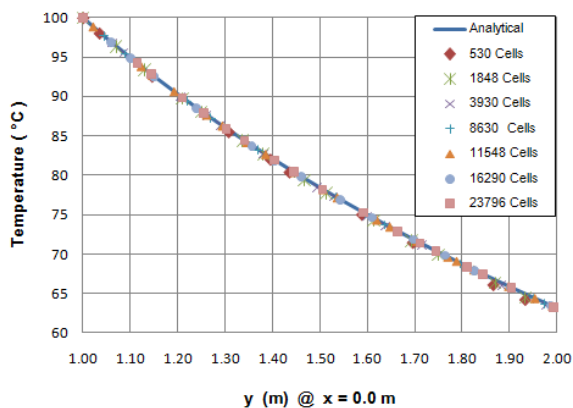


Fig.12 Comparison of temperature for Case C

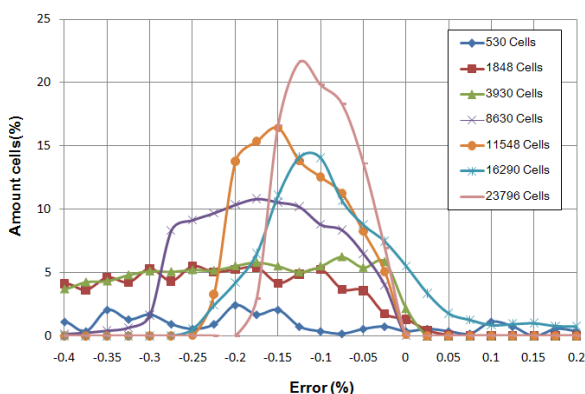


Fig.13 Error distribution of Case C

### 3.4 Case D: Diffusion in a Hexagonal Shape

The last test case in the present work is the diffusion in a hexagonal shape. Dimension and

boundary conditions of the considered case are described in Fig.14. The domain of computation here is reduced to a haft part of the hexagonal due to the symmetry shape. The outer top boundary is set with the condition of insulation while the rest boundaries are specified with the several constants of the temperature. The thermal conductivity ( $k$ ) of the hexagonal is set to  $50 \text{ W/m}^{\circ}\text{C}$ .

This problem has been performed on seven grid sets of 697, 900, 2270, 3600, 4467, 6706, and 9903 cell numbers. The distribution of temperature is displayed in Fig.14. It can be seen that the maximum temperature is distributed in the left and right outer zones due to an attachment to the high temperature boundaries. The distributions of the errors are illustrated in Fig.15. It can be seen that the distribution are within the range of  $-0.3\%$  to  $0.3\%$ . The lower density meshing seems to give the negative distributions with a more spread out than the finer ones.

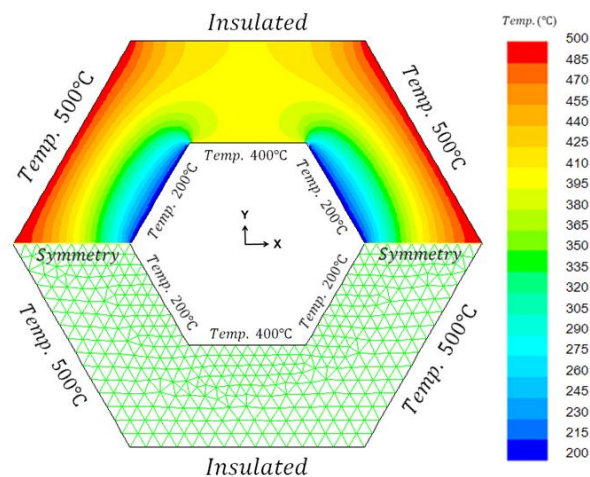


Fig.14 Domain/boundary conditions for Case D

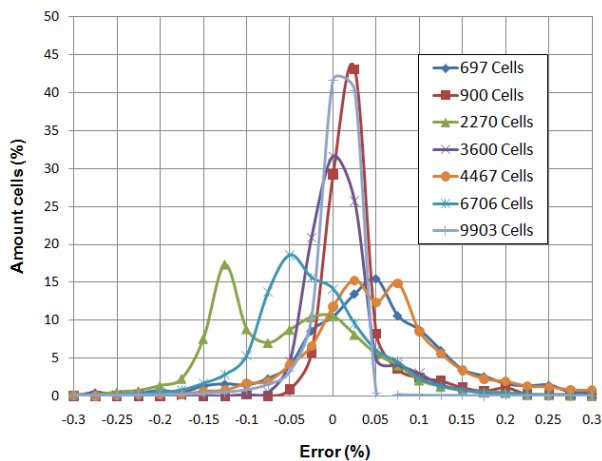


Fig.15 Error distribution of Case D

#### 4. Conclusions

This research work presents the numerical methodology for predicting the two-dimensional diffusion problems. The computer code is developed based on finite volume method and the triangular unstructured meshing is implemented. Four test cases of the diffusion problems are investigated to assess the accuracy in predicting of the developed computer code. The results shown that the developed computer code gives the satisfactory results compare with the analytical solutions.

#### 5. Acknowledgement

The authors are pleased to acknowledge School of Mechanical Engineering, Suranaree University of Technology and National Metal and Material Technology Center (MTEC) for supporting this research work.

#### 6. References

- [1] Versteeg, H.K and Malalasekera, W. (2007). An Introduction to Computational Fluid Dynamic : The Finite Volume Method, 2<sup>nd</sup> edition, Pearson Prentice Hall, New York. pp. 304-342
- [2] Dennis, G. Zill and Michael, R. Cullen(2000). Advanced Engineering Mathematics, 2<sup>nd</sup> edition, Jones and Bartlett. Pp 704-708

- [3] Yunus, A. Cengel,(2006). Heat and Mass Transfer : A Practical Approach, 3<sup>ed</sup> edition (SI Units), Mc Graw Hill. pp.62-108